

Neuron, Volume 112

Supplemental information

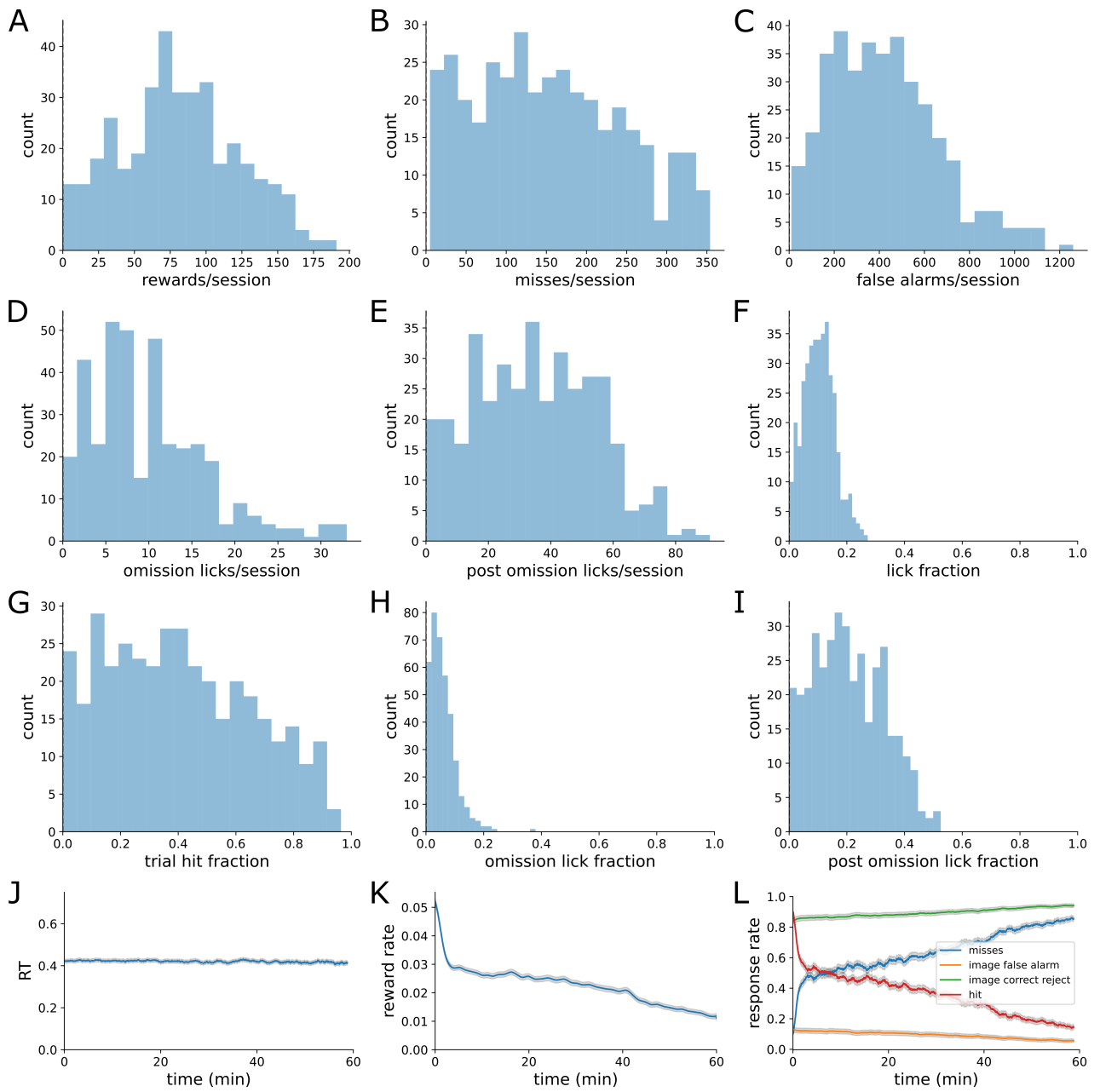
**Behavioral strategy shapes activation
of the Vip-Sst disinhibitory circuit
in visual cortex**

Alex Piet, Nick Ponvert, Douglas Ollerenshaw, Marina Garrett, Peter A. Groblewski, Shawn Olsen, Christof Koch, and Anton Arkhipov

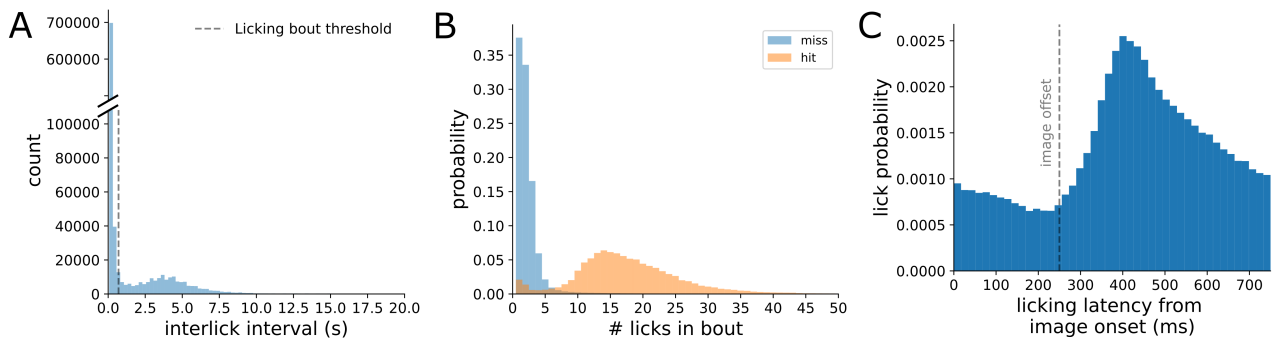
Supplemental Materials

The supplementary materials contains extended figures and control analyses for several aspects of the study:

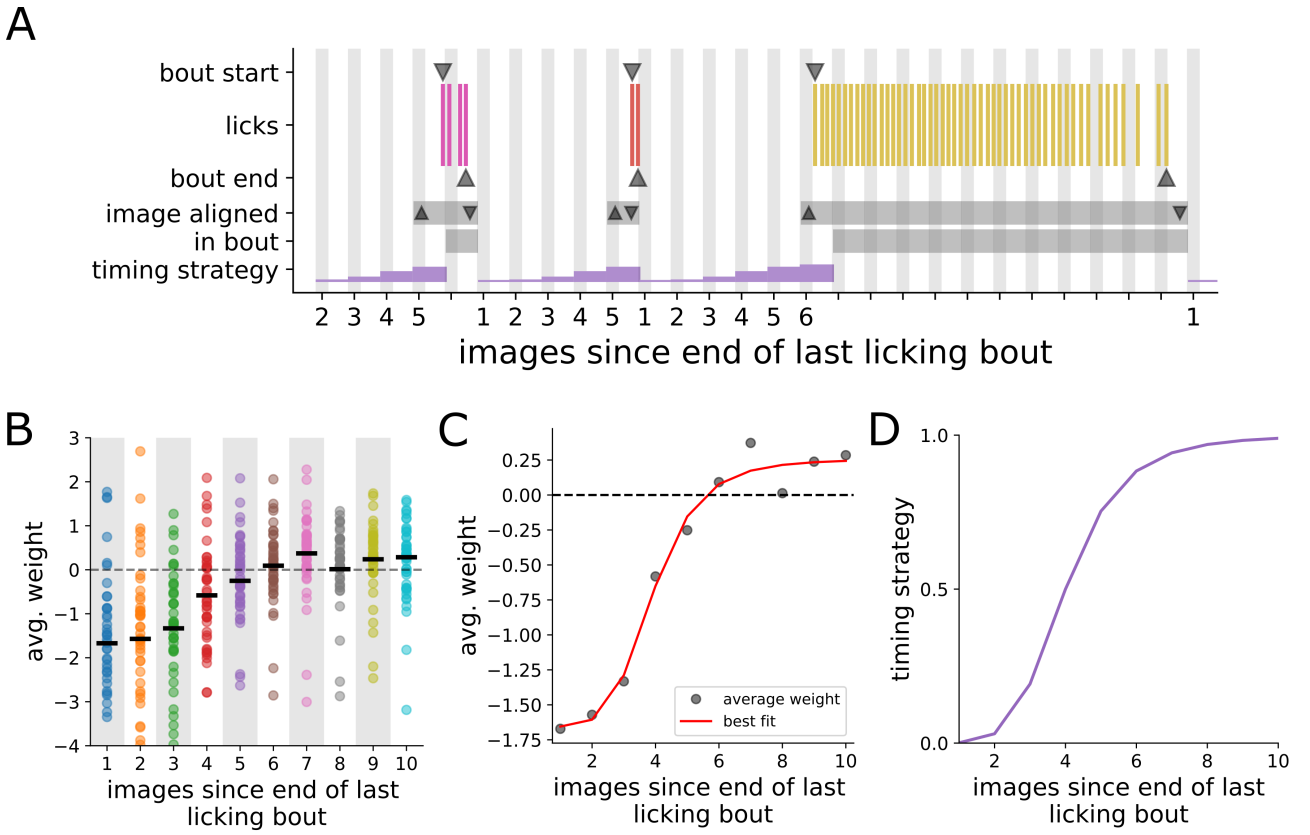
- Fig. S1. Quantification of mouse behavior, related to Figure 1
- Fig. S2. Licks were segmented into licking bouts and aligned to image onset, related to Figure 1
- Fig. S3. Constructing the timing regressor, related to Figure 1
- Fig. S4. Model validation, related to Figure 2
- Fig. S5. Average strategy weights are correlated with task events, related to Figure 2
- Fig. S6. Principal Components Analysis (PCA) on strategy index, related to Figure 2
- Fig. S7. Strategy over training, related to Figure 2
- Fig. S8. Strategy behavior over time, related to Figure 2
- Fig. S9. Analysis of engagement, related to Figure 3
- Fig. S10. Comparing neural activity in V1 and LM, related to Figure 4
- Fig. S11. Strategy differences in response to hits are not due to reward signals, related to Figure 4
- Fig. S12. Neural correlates of behavioral strategy aligned to false alarms, related to Figure 4
- Fig. S13. Licking rates aligned to task events, related to Figure 4
- Fig. S14. Pupil diameter aligned to task events, related to Figure 4
- Fig. S15. Distribution of running speeds split by strategy and transgenic line, related to Figure 4
- Fig. S16. Running speeds aligned to task events, related to Figure 4
- Fig. S17. Running matched Vip mice, related to Figure 4
- Fig. S18. Microcircuit dynamics, related to Figure 5
- Fig. S19. Running speed and task engagement, related to Figure 7
- Fig. S20. Stimulus novelty has a small influence on strategy, related to Figure 4
- Fig. S21. Both dominant strategies show robust changes to novel stimuli, related to Figure 4
- Fig. S22. False alarm decoding, related to Figure 6



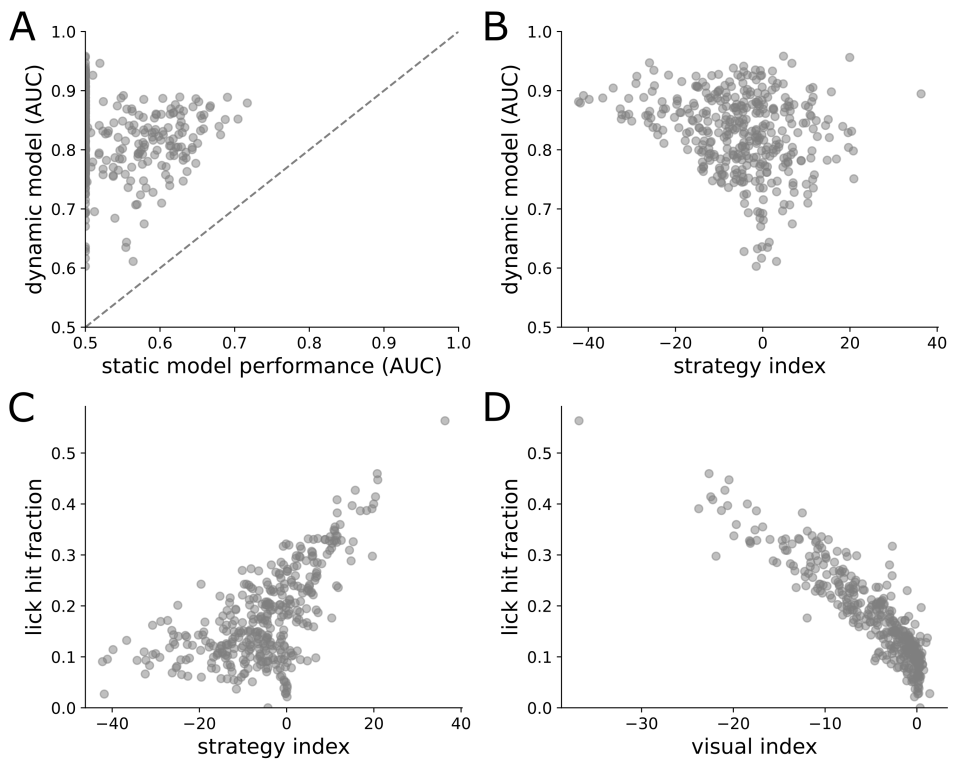
Supplementary Figure 1: **Quantification of mouse behavior, related to Figure 1.** (A) Histogram of rewards/session. (B) Histogram of misses/session. (C) Histogram of false alarms / session. (D) Histogram of omissions with licks/session. (E) Histogram of post-omission-licks/session (F) Histogram of average lick fraction per session. (G) Histogram of fraction of image changes with licks per session. (H) Histogram of fraction of omissions with licks per session. (I) Histogram of fraction of post-omission images with licks per session. (J) Average Response latency over time. (K) Average reward rate over time. (L) Hit, Miss, False alarm, and correct reject rates over time.



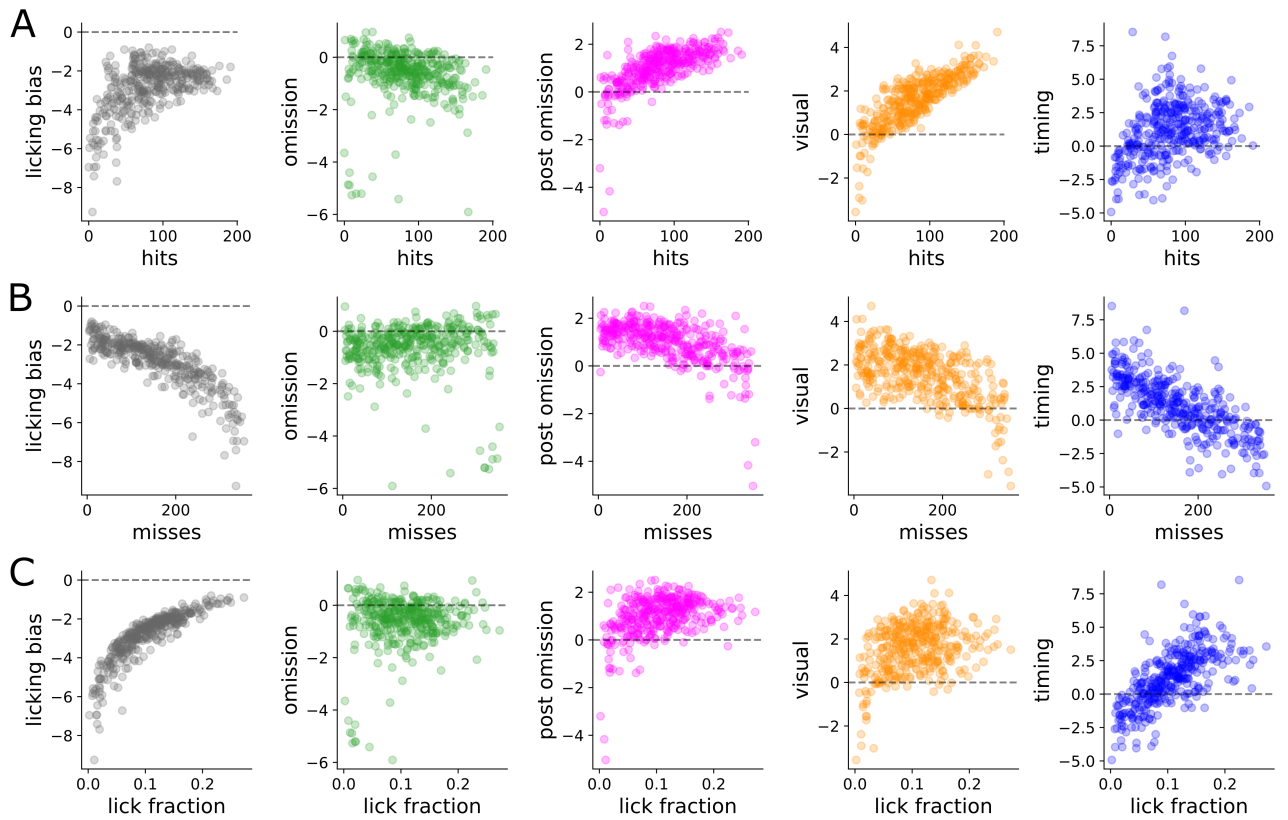
Supplementary Figure 2: Licks were segmented into licking bouts and aligned to image onset, related to Figure 1. (A) Histogram of interval between successive licks ($n = 936,136$ licks from 382 imaging sessions). Dashed line indicates 700 ms threshold used to separate licks within the same licking bout ($< 700\text{ms}$) and licks in separate licking bout ($> 700\text{ ms}$). (B) Histogram of the number of licks in each licking bout separated by whether the licking bout earned a reward (hit) or did not (miss) ($n = 190,410$ licking bouts from 382 imaging sessions). (C) Histogram of the response latency for the start of each licking bout with respect to the most recent image onset ($n = 190,410$ licking bouts from 382 imaging sessions).



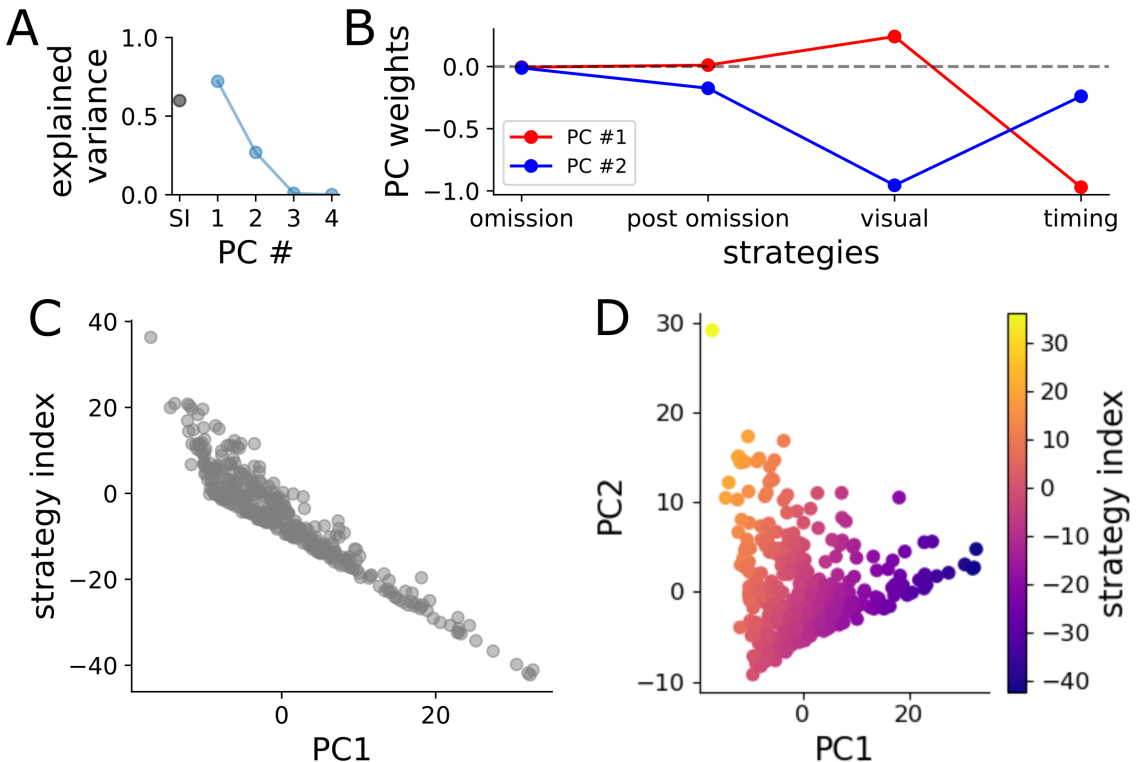
Supplementary Figure 3: Constructing the timing regressor, related to Figure 1. (A) Schematic illustrating how timing is measured. Shaded bars indicate the time of stimulus presentations. Tick marks indicate the time of each lick. Individual licking bouts are colored separately. Down arrows (∇) indicate the start of each licking bout. Up arrows (Δ) indicate the end of each licking bout. Our model predicts whether the mouse will start a licking bout on each image presentation. Therefore images where the mouse was already in a licking bout are excluded from the fitting process. Consequently, our timing regressor starts measuring how many images have been presented since the end of the last licking bout starting at 1. The timing strategy is a sigmoidal function of time since the end of the last licking bout. Note the timing strategy is undefined on images when the mouse was already in a licking bout. (B) A subset of 45 sessions were used to construct the timing regressor. The strategy model was fit with 10 timing regressors, each using 1-hot encoding for different length delays since the image with the end of the last licking bout. Average weight of each 1-hot timing regressor (dots, $n=45$ sessions) Black bars indicate the average across sessions. (C) A four parameter sigmoid was fit to the average regressor weights from panel B (gray dots). The best fitting sigmoid is shown in red. (D) The timing strategy uses the midpoint and shape parameters from panel C, but scales the sigmoid to unit height. The strategy vector is later mean-centered.



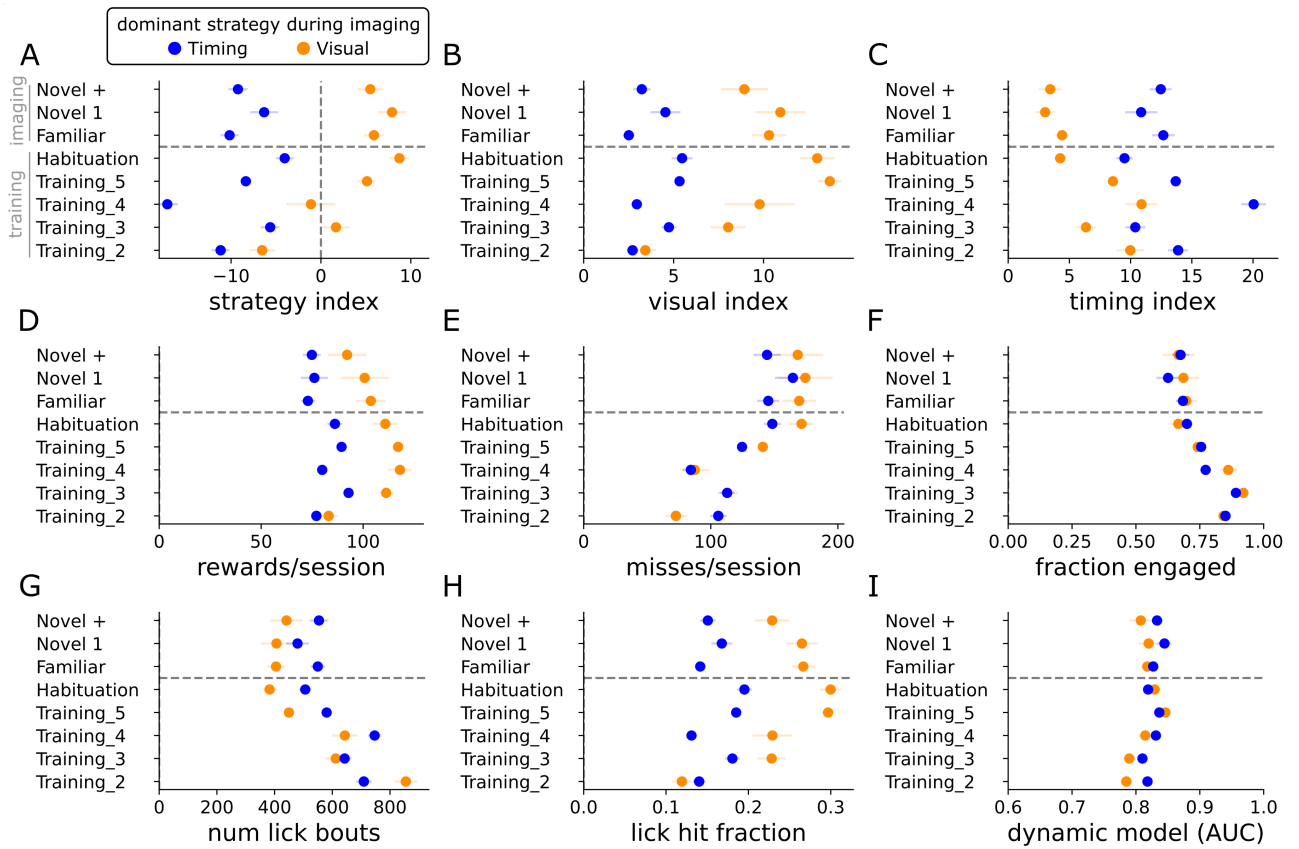
Supplementary Figure 4: **Model validation, related to Figure 2.** (A) Scatter plot of area under ROC curves for each session for the dynamic model compared to static logistic regression ($n=382$ imaging sessions). Dashed line marks unity. (B) Scatter plot of area under ROC curves for each session for the dynamic model compared to the strategy index. (C-D) The lick hit fraction is the fraction of licking bouts that resulted in a reward. (C) Lick hit fraction compared to the strategy index. (D) Lick hit fraction compared to the visual strategy index.



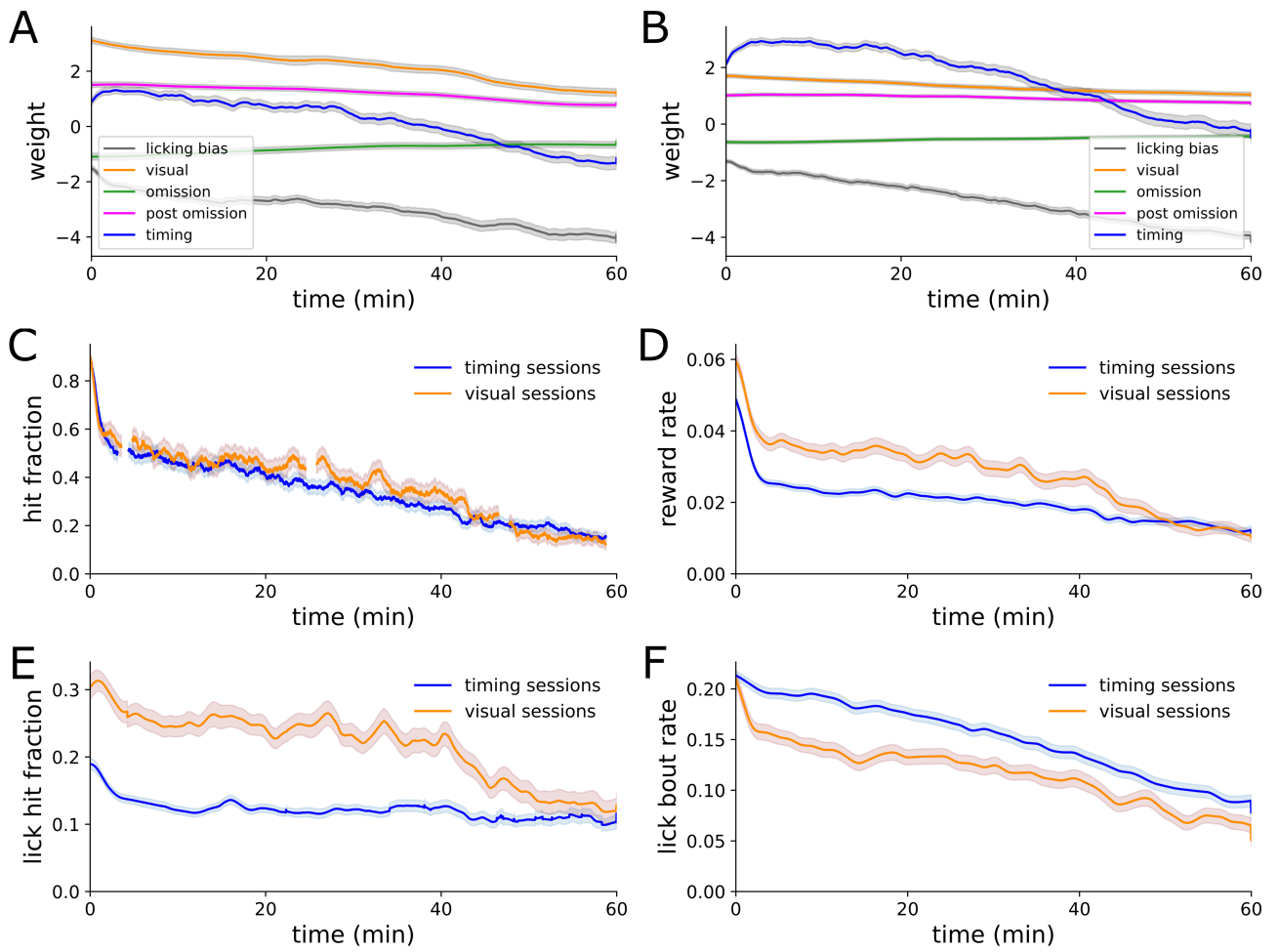
Supplementary Figure 5: **Average strategy weights are correlated with task events, related to Figure 2.** Scatter plot between the average weight of each strategy and task events. Hits (A) are image changes with a reward, misses (B) are image changes without a reward, and lick fraction (C) is the fraction of images with a lick bout start.



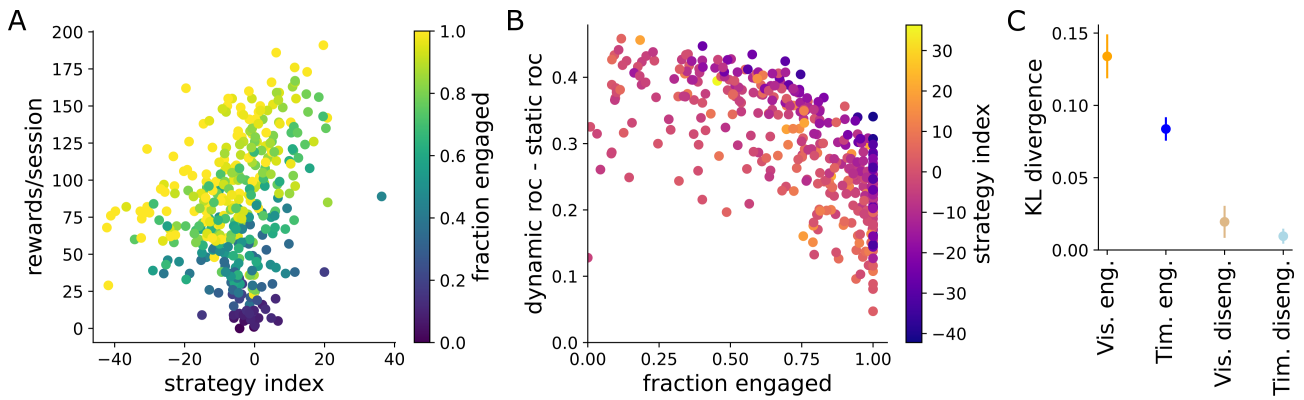
Supplementary Figure 6: **Principal Components Analysis (PCA) on strategy scores, related to Figure 2.** To assess the variability of strategies across our behavioral dataset we performed PCA on the matrix containing the fractional reduction in model evidence after removing each strategy, for each of the 382 imaging sessions. (A) Variance along each principal component (PC #), as well as the variance along the strategy index (SI). The top two components contain 99.04% of the total variance (72.13% and 26.90%, respectively). 98.24% of all variance is contained in just the timing and visual strategy indices. The strategy index, which is simply the difference between the visual and timing indices, contains 59.95% of the total variance, and has a strong correlation with the top principal component ($R^2 = 0.88$). (B) The top two principal components are aligned with the timing and visual strategies, respectively. (C) Scatter plot between each session projected onto the first principal component and the strategy index. (D) All sessions (n=382 imaging sessions) projected onto the first two principal components and colored by the strategy index.



Supplementary Figure 7: Strategy over training, related to Figure 2. We classified mice by their dominant strategy (visual or timing) based on their behavior during imaging. We then fit our strategy model to the training sessions and examined how their strategy preferences changed over training. Metrics as described in Figure S1. Training steps described in the STAR methods, and in.¹ We did not fit the model to training stages 0 and 1 because the stimulus was continuous and not periodically presented. Each dot shows mean +/- SEM for each strategy group. n= 252 sessions in Training-2, 239 Training-3, 331 Training-4, 1059 Training-5, 270 Habituation, 187 Familiar, 66 Novel 1, 123 Novel+. (A-C) Visual mice increase their use of the visual strategy over training, while decreasing their use of the timing strategy. (D) Rewards per session for both strategies. (E) The number of missed images increase over training for both strategies. (F) Both strategies decrease the fraction of the session in which they are engaged. (G) Both strategies show decreases in the number of licking bouts. (H) The fraction of licking bouts that result in a reward. As mice increase their lick hit fraction, they need to lick less often to earn the same number of rewards. By increasing their lick hit fraction, this means they are licking on image changes more often rather than licking early which delays the next image change. Increasing their lick hit fraction means they can earn more rewards in less time, and thus they disengage earlier and miss more image changes while they are disengaged. (I) Strategy model fit performance (area under ROC curve).

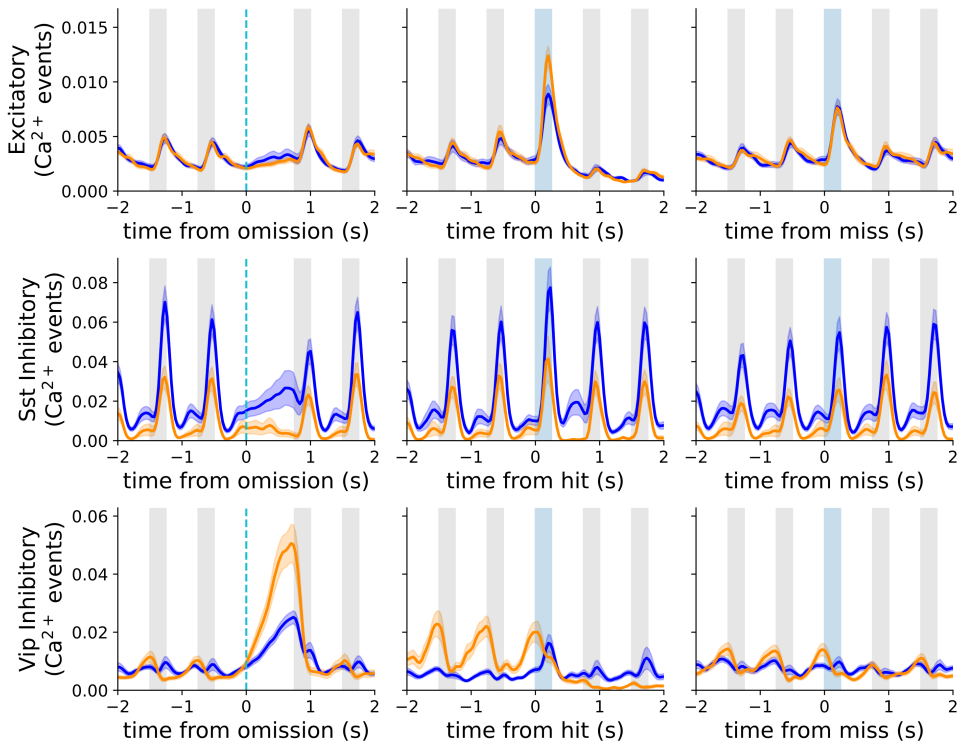


Supplementary Figure 8: **Strategy behavior over time, related to Figure 2.** (A) Average strategy weights over time for visual strategy sessions ($n = 116$ sessions). (B) Same as A but restricted to timing strategy sessions ($n=260$ sessions). (C) Hit fraction split by visual or timing strategy sessions. (D) Reward rate split by visual or timing strategy sessions. (E) Lick hit fraction split by visual or timing strategy sessions. (F) Lick bout rate split by visual or timing strategy sessions.

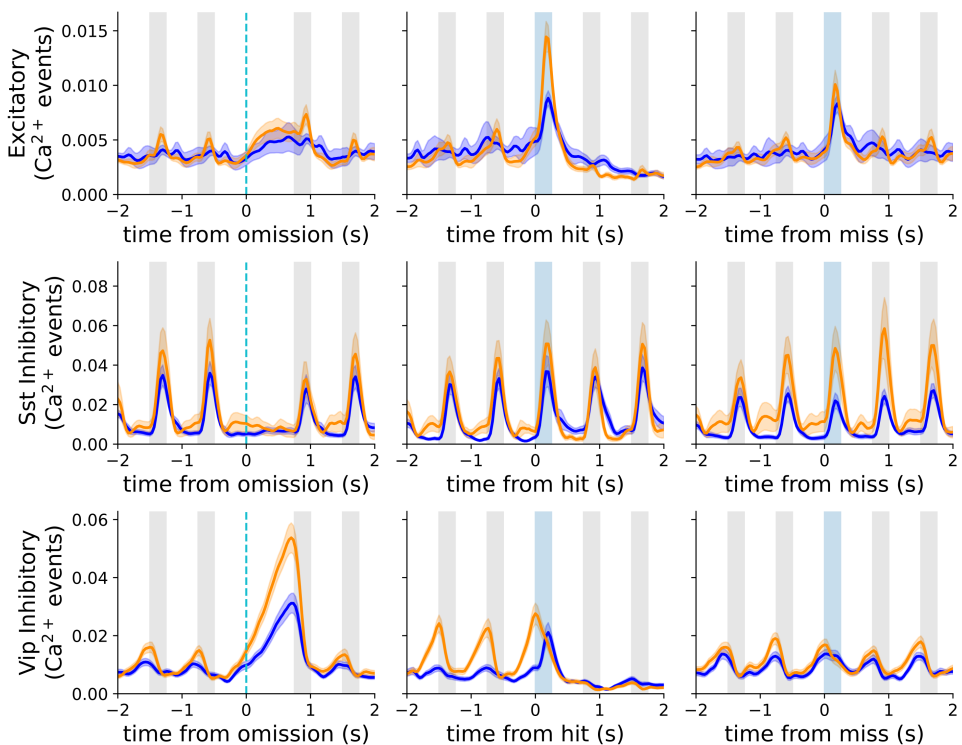


Supplementary Figure 9: **Analysis of engagement, related to Figure 3.** (A) Scatter plot of rewards per session against the strategy index, color scale shows the fraction of each session in which the mouse was engaged ($n= 376$ sessions). (B) Scatter plot of the difference in model performance between the dynamic and static models against the fraction of each session in which the mouse was engaged. The color scale shows the strategy index ($n=376$ sessions). (C) KL divergence between a uniform distribution and response time distributions for each combination of strategy and engagement state (Fig. 3G,H). Error bars show SEM estimated with a hierarchical bootstrap over behavioral sessions with 10,000 bootstrap iterations.

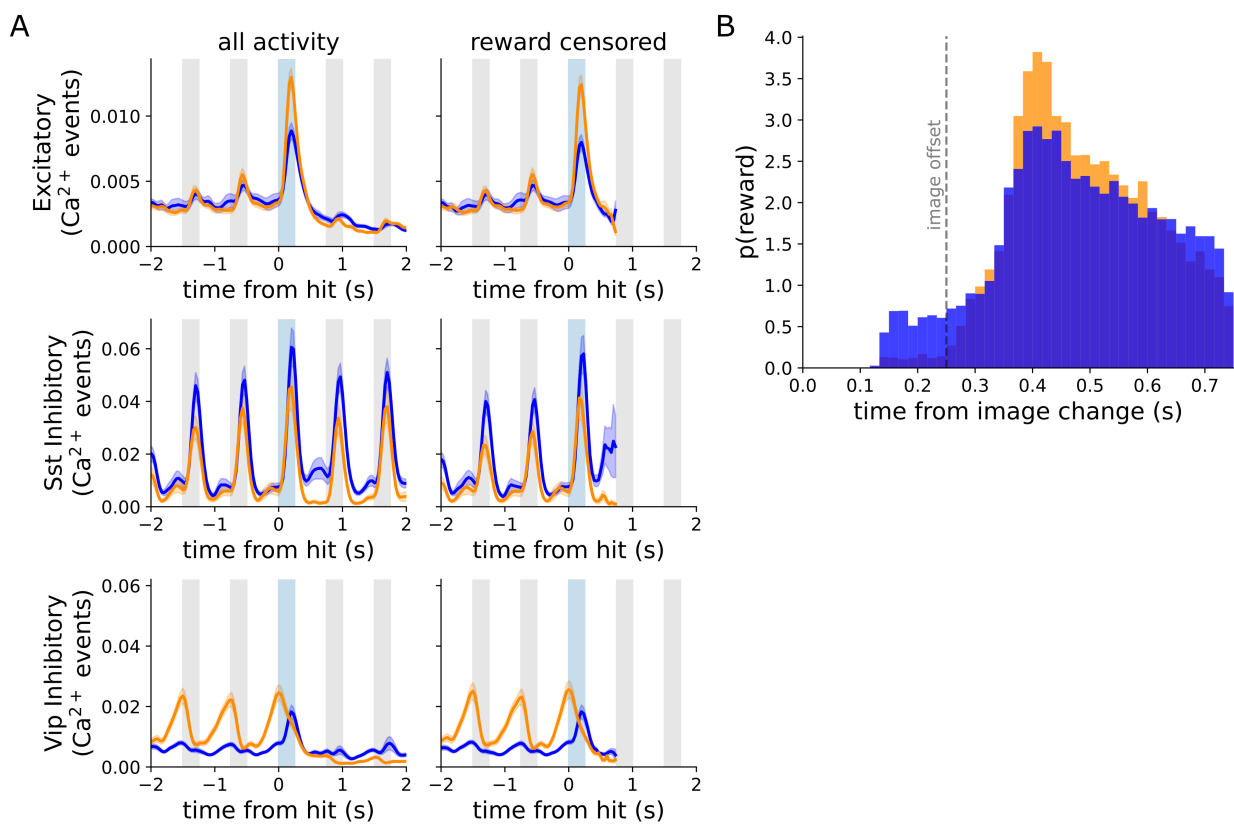
A. V1



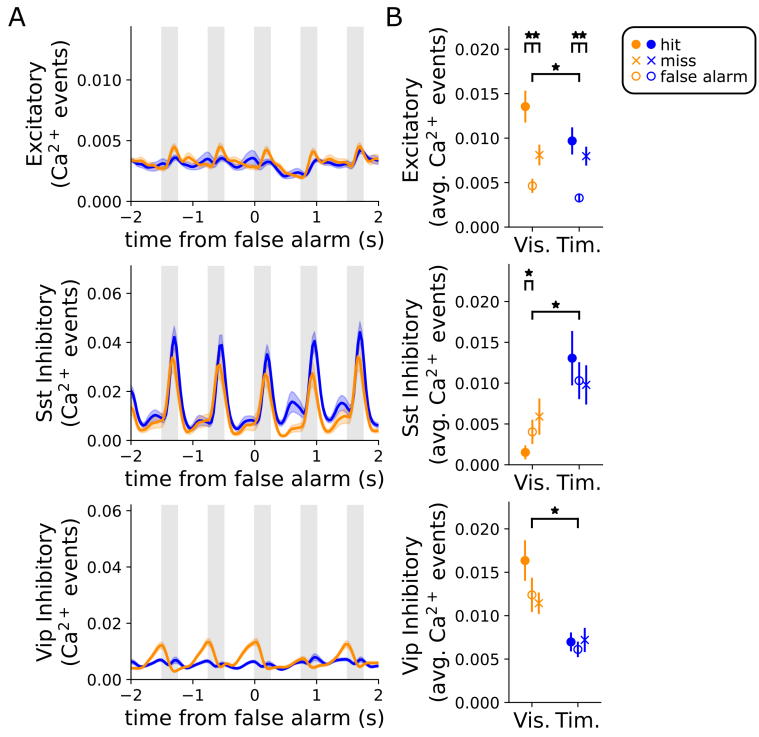
B. LM



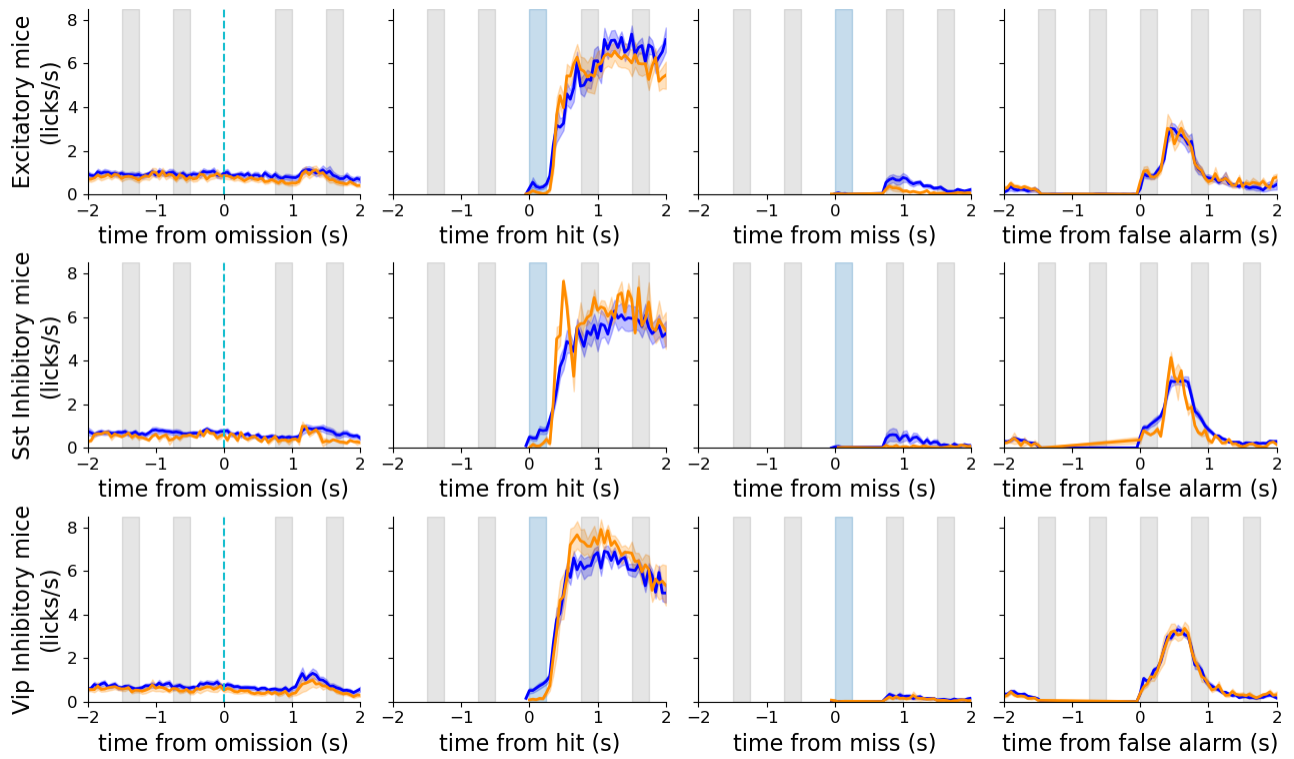
Supplementary Figure 10: Comparing neural activity in V1 and LM, related to Figure 4. Average calcium event magnitude of each cell class aligned to omissions, hits, and misses, split by the dominant behavioral strategy and cortical area. (A) Cells from V1 (n=5,734 Excitatory; 282 Sst inhibitory; 604 Vip inhibitory cells). (B) Cells from LM (n=2,885 Excitatory; 188 Sst inhibitory; 635 Vip inhibitory cells).



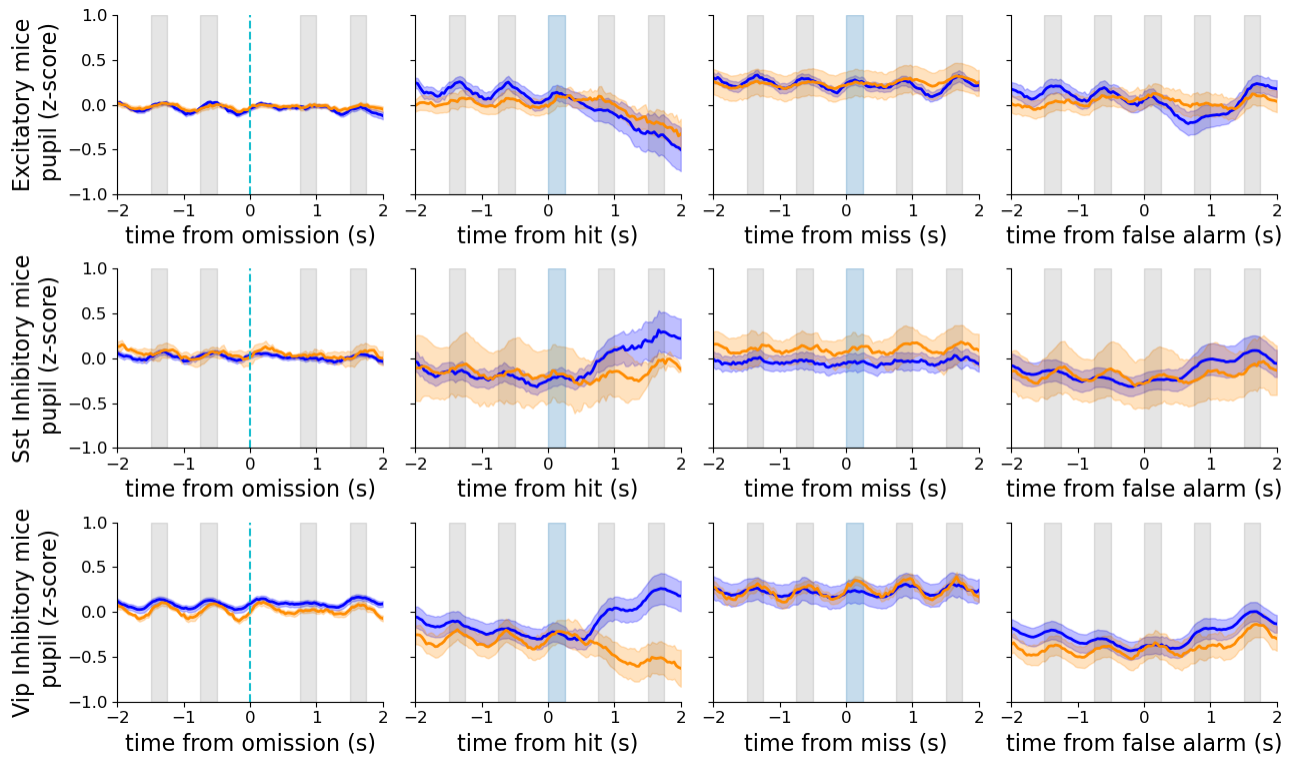
Supplementary Figure 11: Strategy differences in response to hits are not due to reward signalling, related to Figure 4. Rewards are delivered at the time of the first valid lick after the image change. Licks in the interval (0, 150 ms) after the image change are ignored. (A) Average calcium event magnitude of each cell class aligned to hits split by the dominant behavioral strategy. The left column shows all activity (same as Fig. 4D). The right column shows reward censored neural activity, that is only neural activity that occurred before the time of reward on each trial. All rewards happen before the subsequent image is displayed (at 750 ms). (B) Histogram of reward times with respect to image changes split by the dominant behavioral strategy.



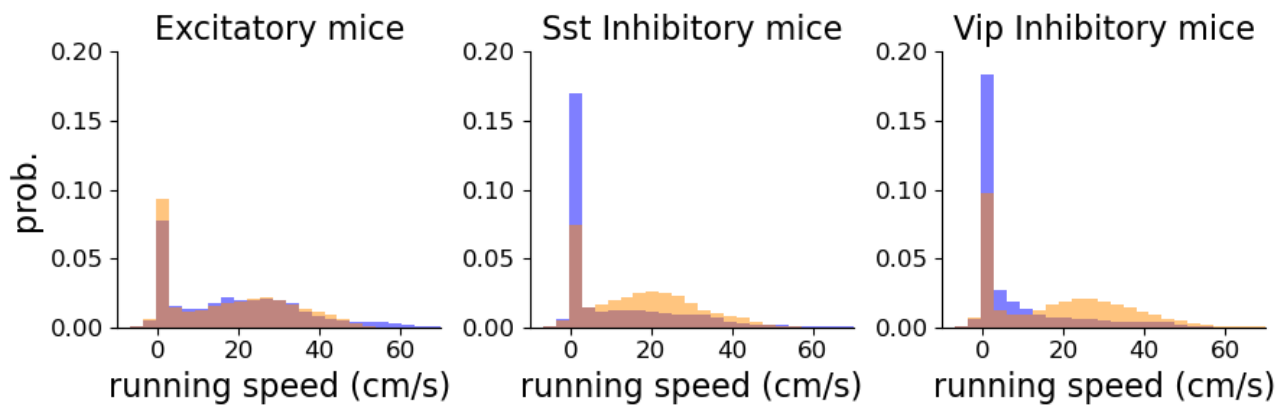
Supplementary Figure 12: Neural correlates of behavioral strategy aligned to false alarms, related to Figure 4. (A) Average calcium event magnitude of each cell class aligned to false alarms split by dominant behavioral strategy. (B) Average calcium event magnitude $\pm/-$ hierarchically bootstrapped SEM in an interval around image changes split by strategy for hits, misses, and false alarms. Hit and miss data are the same as Fig. 4E. Excitatory and Sst cells show average events after the image presentations (150, 250 ms) and (375, 750 ms) respectively. Vip cells show average events immediately before image presentations (-375, 0 ms). * indicates $p < 0.05$ from a hierarchical bootstrap over imaging planes and cells, corrected for multiple comparisons. Significance tests are only shown for false alarm responses for clarity. (Excitatory) We do not observe increased activity during false alarms for cells from either strategy (visual FA 0.0046 ± 0.00070 , timing FA 0.0033 ± 0.00037 , visual FA vs hit $p = 0$, visual FA vs miss $p = 0.0014$, timing FA vs hit $p = 0$, timing FA vs miss $p = 0$). Cells from visual strategy sessions showed elevated activity compared to cells from timing strategy sessions (visual FA 0.0046 ± 0.00070 , timing FA 0.0033 ± 0.00037 , $p = 0.031$). (Sst) Both strategy sessions showed intermediate levels of activity after false alarms compared to hits and misses. The difference in activity was only significant between visual hits and false alarms (visual FA 0.0040 ± 0.0014 , visual FA vs hit $p = 0.043$). Cells from visual strategy sessions showed decreased activity compared to cells from timing strategy sessions (visual FA 0.0040 ± 0.0014 , timing FA 0.010 ± 0.0021 , $p = 0.0043$). (Vip) Cells from visual strategy sessions show elevated activity before false alarms compared to cells from timing strategy sessions (visual FA 0.0124 ± 0.0019 , timing FA 0.0061 ± 0.00078 , $p = 0.00020$). Vip activity before false alarms was not significantly different from activity before hits or misses for either strategy. However the difference between hits and false alarms for cells from visual strategy sessions was close to significance (visual FA 0.0124 ± 0.0019 , $p = 0.086$).



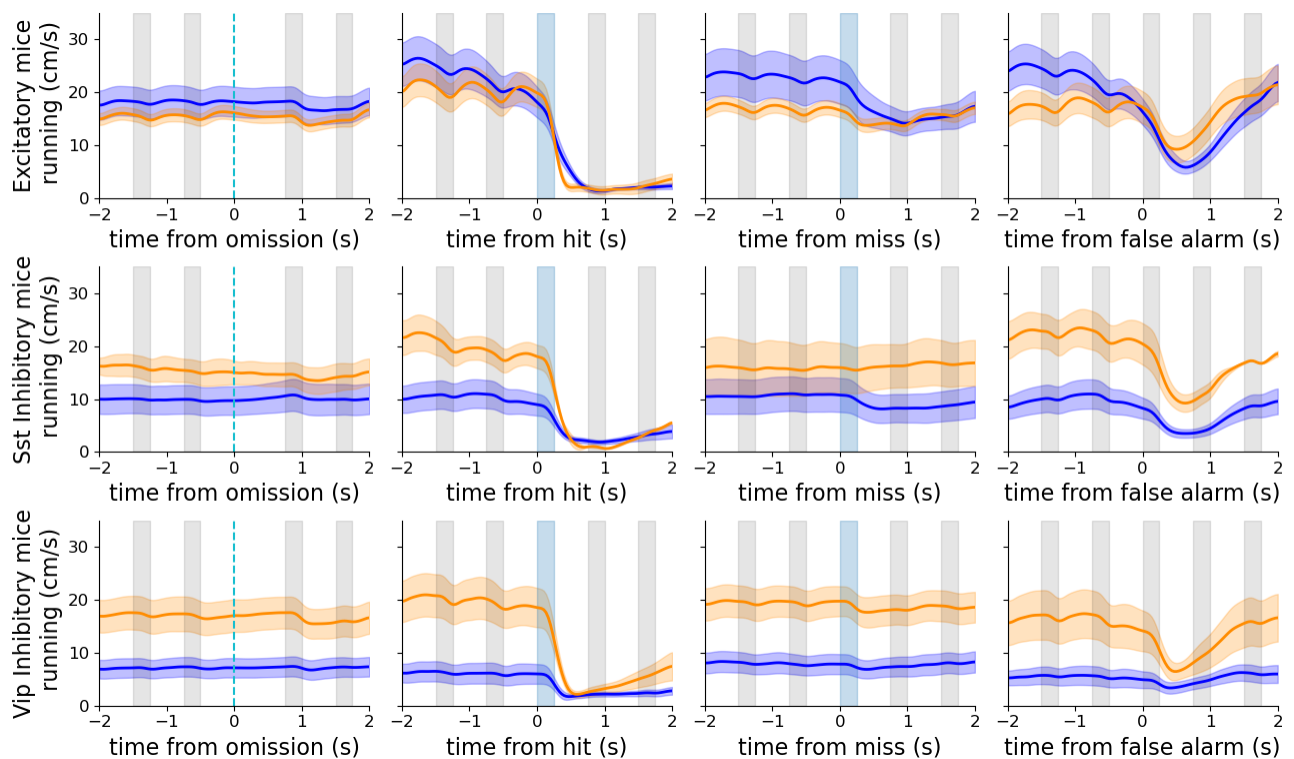
Supplementary Figure 13: **Licking rates aligned to task events, related to Figure 4.** Licking rates are shown for each transgenic mouse line separately to facilitate interpretation of neural data. Rates are averages +/- SEM over behavioral sessions (Exc, 21 sessions from 9 mice. Sst, 15 sessions from 6 mice. Vip, 21 sessions from 9 mice). Individual licks were binned into 50ms time bins relative to task events. The average lick rate for each session was computed and then combined across sessions.



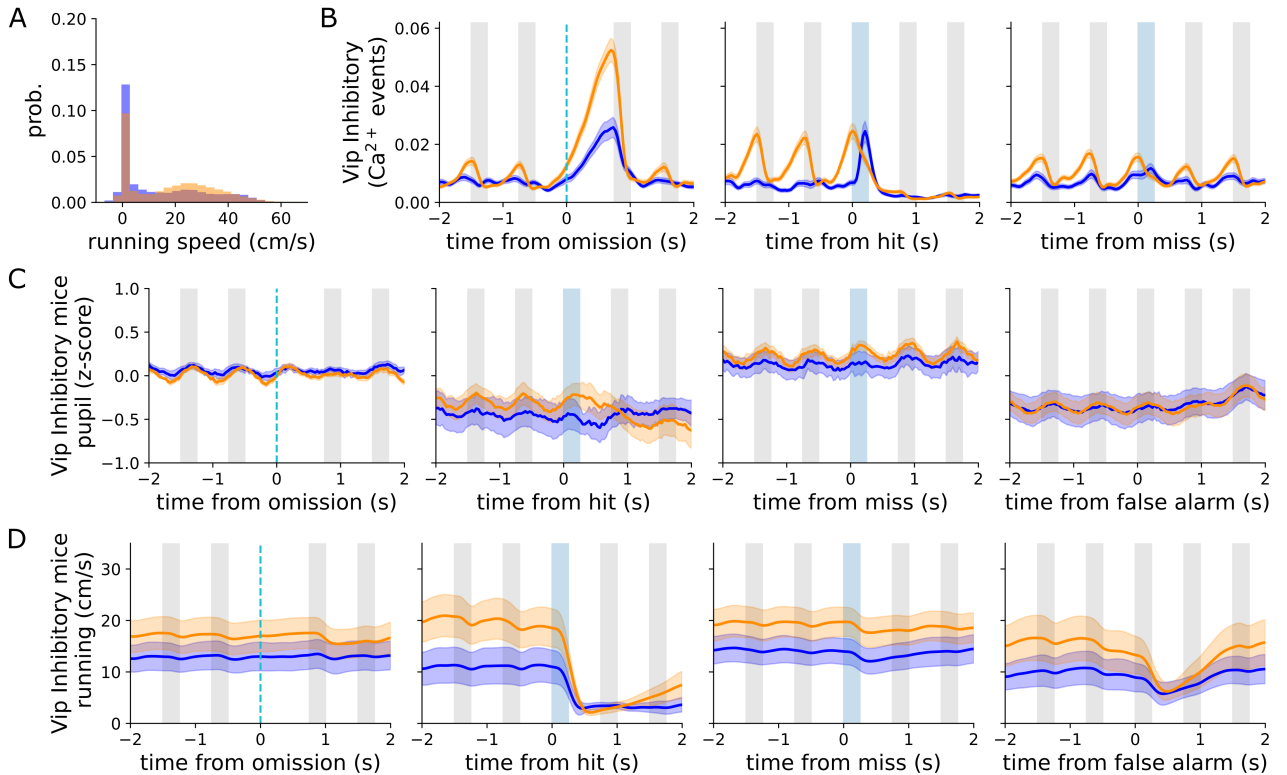
Supplementary Figure 14: Pupil diameter aligned to task events, related to Figure 4. Z-scored average pupil dynamics are shown for each transgenic mouse line separately to facilitate interpretation of neural data. Plots are averages \pm SEM over behavioral sessions (Exc, 21 sessions from 9 mice. Sst, 15 sessions from 6 mice. Vip, 21 sessions from 9 mice). For each session, we first z-scored the pupil diameter trace and removed time points with $z > 2$ or $z < -2$. After removing the outliers we z-scored the original time series, and computed the average for each behavioral session. We then combined the average pupil traces across sessions.



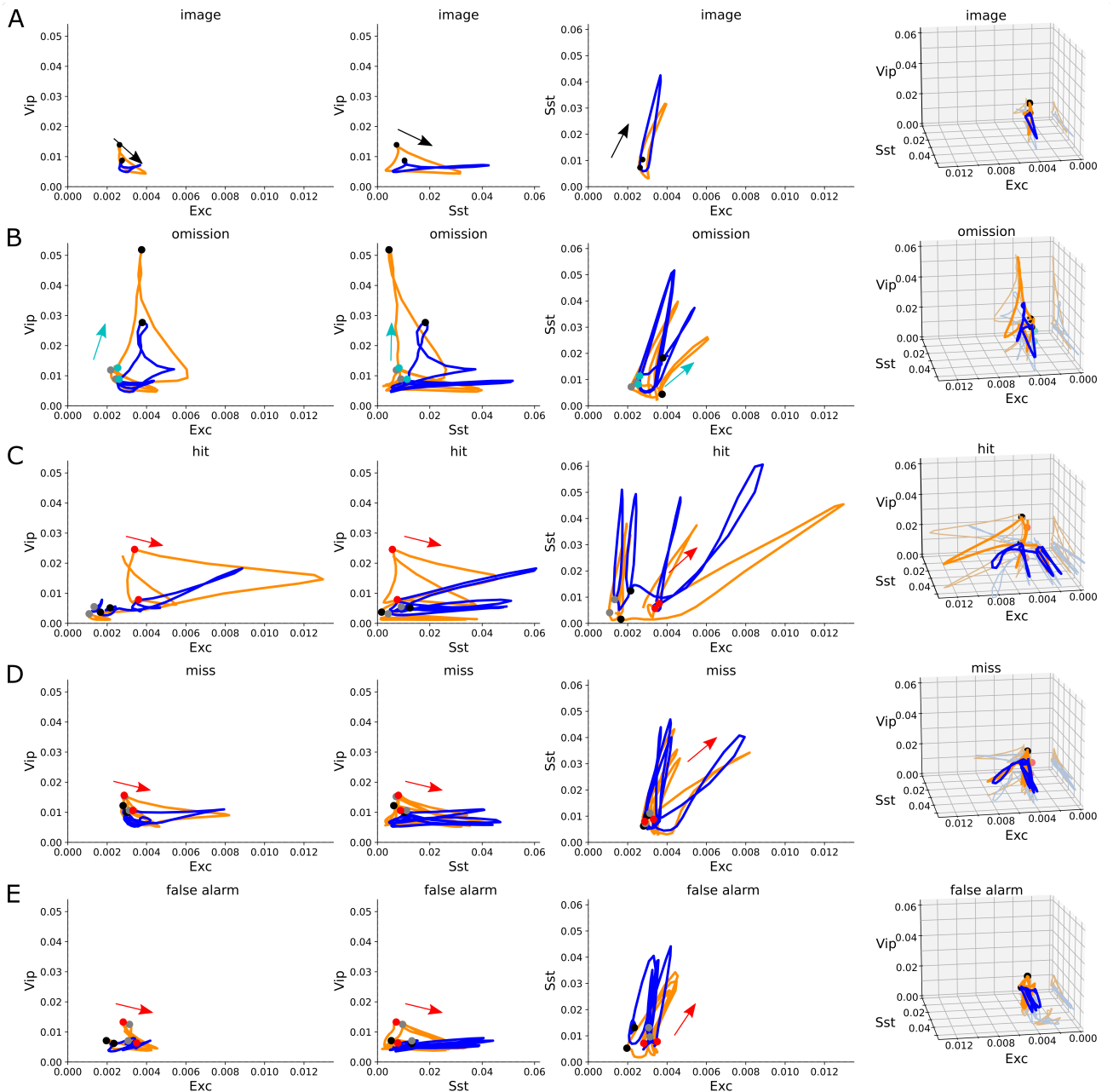
Supplementary Figure 15: **Distribution of running speeds split by strategy and transgenic line, related to Figure 4.** Running speeds are shown split by transgenic mouse lines to facilitate interpretation of neural data. For each strategy we show the combined distribution of running speeds across all mice. For each session we get the average running speed during each 750 image interval, resulting in 4800 time points per session.



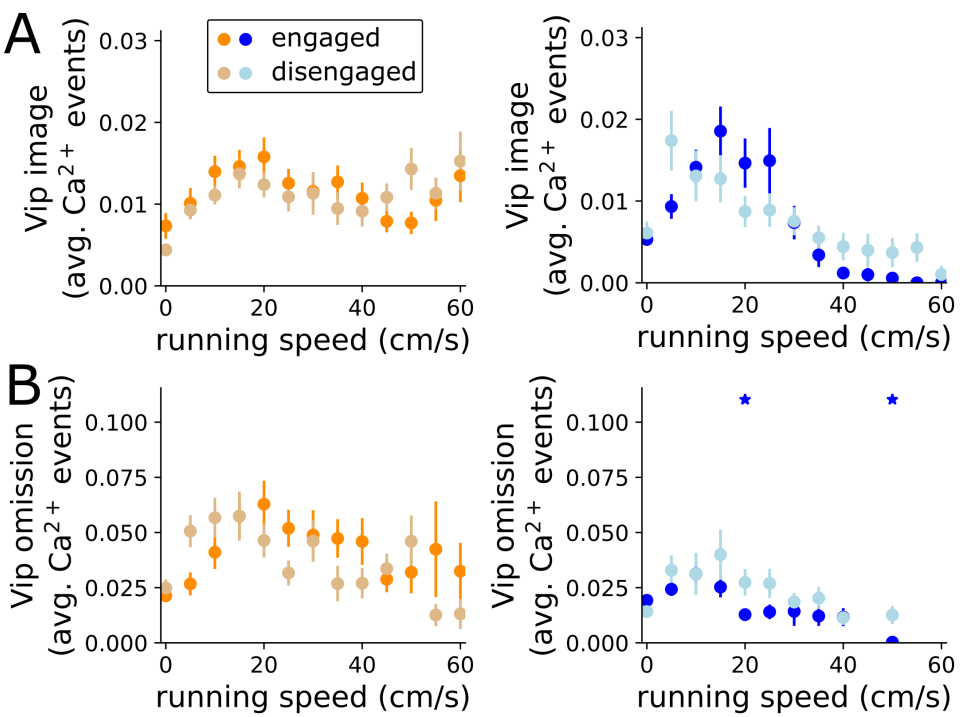
Supplementary Figure 16: **Running speeds aligned to task events, related to Figure 4.** Average running speeds for each transgenic mouse line are shown separately to facilitate interpretation of neural data. Plots are averages +/- SEM over behavioral sessions (Exc, 21 sessions from 9 mice. Sst, 15 sessions from 6 mice. Vip, 21 sessions from 9 mice). For each session we computed the average running speed aligned to each task event, and then combined across sessions.



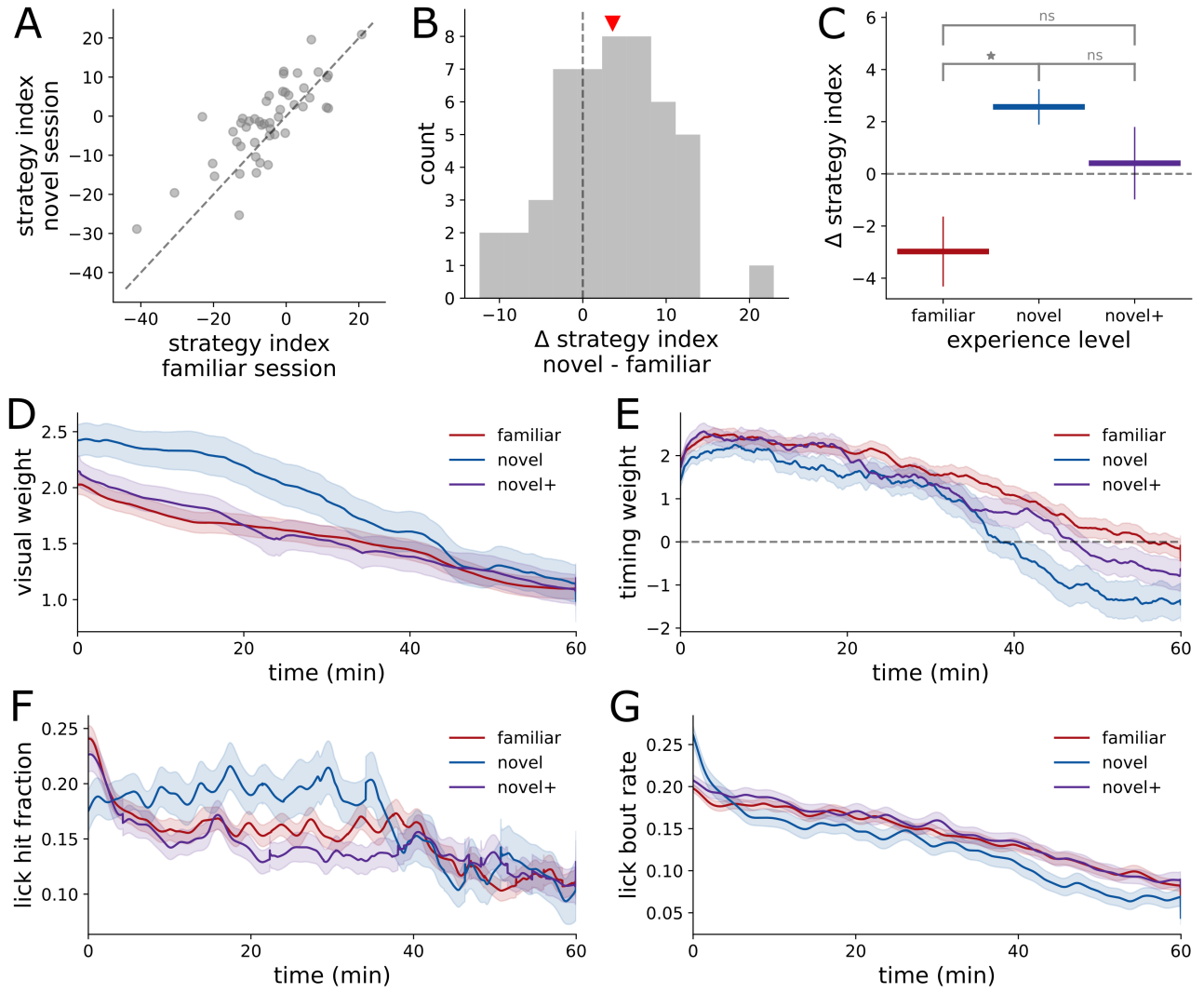
Supplementary Figure 17: **Running matched Vip mice, related to Figure 4.** Three timing strategy mice with low running speeds were removed; we refer to the remaining mice as running matched. (A) Distribution of running speeds in the running matched dataset. The distributions are not perfectly matched but are much closer than the general dataset. (B) Average Vip population neural activity aligned to task events for the running matched mice. (C) Average z-score pupil diameter aligned to task events for the running matched mice. (D) Average running speed aligned to task events for the running matched mice.



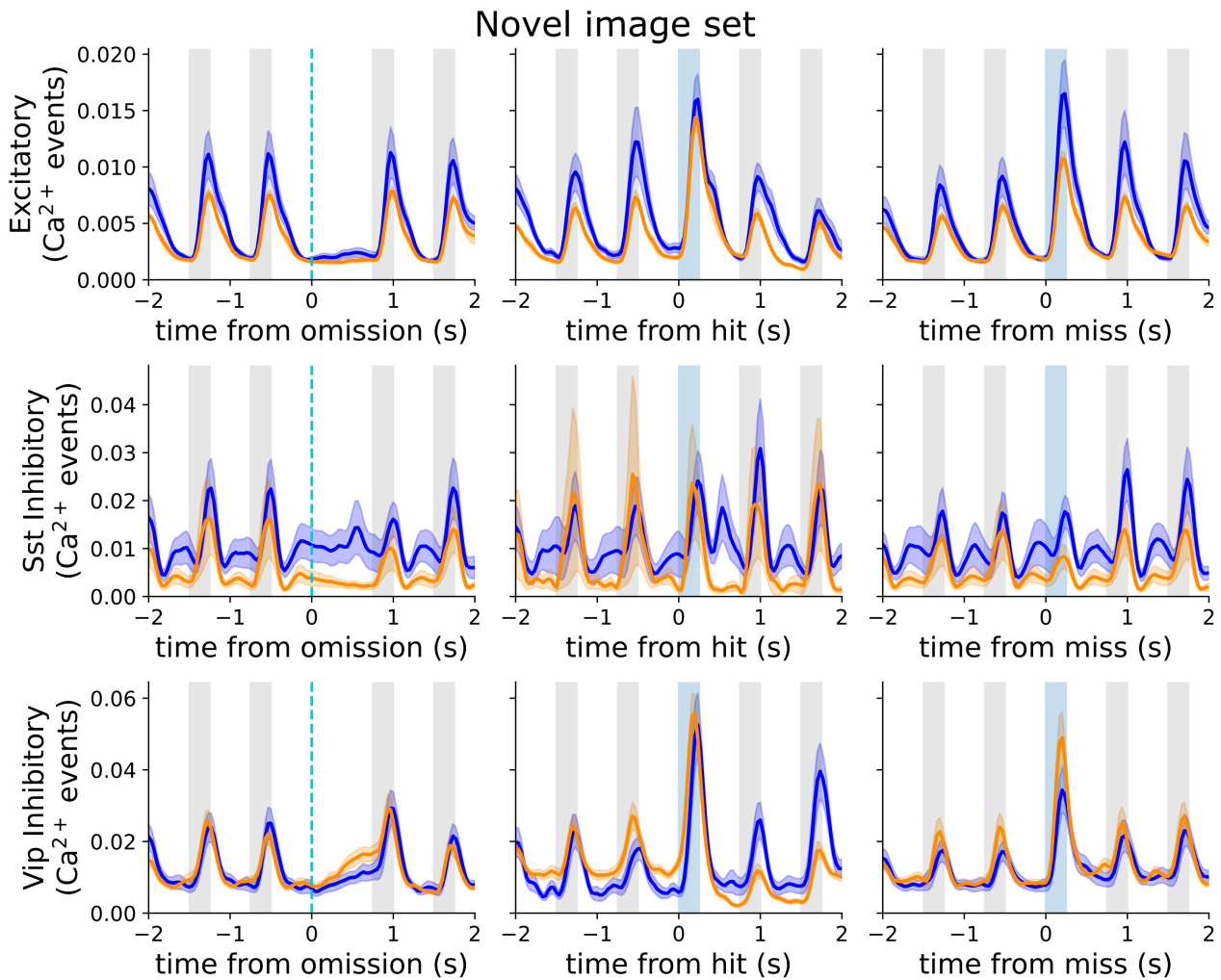
Supplementary Figure 18: **Microcircuit dynamics, related to Figure 5.** Average population activity of different cell classes plotted against each other, similar to figure 5D, in response to (A) image repeats, (B) image omissions, (C) hits, (D) misses, and (E) false alarms.



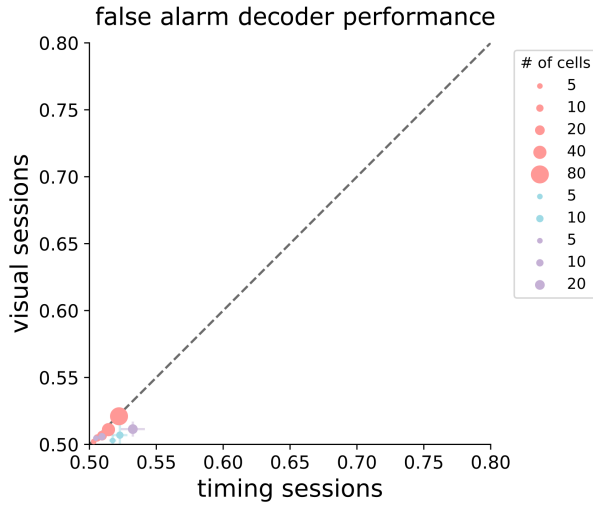
Supplementary Figure 19: **Running speed and task engagement, related to Figure 7.** Similar to 4F,G. Vip activity in response to images and omissions across running speeds split by dominant strategy and task engagement. Stars indicates $p < 0.05$ after a hierarchical bootstrap across imaging planes and cells, then corrected for multiple comparisons.



Supplementary Figure 20: **Stimulus novelty has a small influence on strategy, related to Figure 4.** The mice were trained on one set of 8 images, we refer to this as the familiar image set. After imaging during the familiar image set, the mice were transitioned to a new set of 8 images termed here as novel image set. We compare how this transition influenced mouse strategy. The familiar session is the last session using the familiar image set. Novel is the first exposure to the new image set. Novel+ is a repeated exposure to the new image set. The transition to novel stimuli is explored in-depth in Garrett et al, 2023.¹ (A) Scatter plot of the strategy index for familiar and novel sessions. Each dot is a pair of sessions from the same mouse. (B) Histogram of the difference between strategy index on the novel session compared to the familiar session. (C) Average value of the strategy index across all mice relative to each mouse's average strategy index value. Significance determined with a paired t-test, $p < 0.05$. ($n = 187$ familiar sessions, 66 novel sessions, 123 novel+ sessions) (D) Visual strategy weight over time split by experience level. (E) Same as D but for the timing strategy weight. (F) Lick hit fraction over time split by experience level. (G) Lick bout rate split by experience level.



Supplementary Figure 21: Both dominant strategies show robust changes to novel stimuli, related to Figure 4. Cells from mice performing both strategies show the effects of novelty explored in Garrett et al, 2023.¹ Average population activity on sessions with novel stimuli for each cell class split by strategy aligned to either image omissions (left), hits (center), or misses (right). Compare with figure 4D, which show population activity on sessions with familiar stimuli.



Supplementary Figure 22: **False alarm decoding, related to Figure 6.** Similar to Figure 6C. Decoding was performed on neural activity in the first 400ms after image presentations. Error bars are SEM over image planes. Each cell type is plotted as a separate color with marker size indicating the number of cells used for decoding from each imaging plane. Markers show cross validated random forest classifier performance at decoding false alarms from the image presentation immediately before the false alarm (% correct, chance is 50%).

References

- Garrett, M., Groblewski, P., Piet, A., Ollerenshaw, D., Najafi, F., Yavorska, I., Amster, A., Bennett, C., Buice, M., Caldejon, S., Casal, L., D’Orazi, F., Daniel, S., de Vries, S. E., Kapner, D., Kiggins, J., Lecoq, J., Ledochowitsch, P., Manavi, S., Mei, N., Morrison, C. B., Naylor, S., Orlova, N., Perkins, J., Ponvert, N., Roll, C., Seid, S., Williams, D., Williford, A., Ahmed, R., Amine, D., Billeh, Y., Bowman, C., Cain, N., Cho, A., Dawe, T., Departee, M., Desoto, M., Feng, D., Gale, S., Gelfand, E., Gradis, N., Grasso, C., Hancock, N., Hu, B., Hytnen, R., Jia, X., Johnson, T., Kato, I., Kivikas, S., Kuan, L., L’Heureux, Q., Lambert, S., Leon, A., Liang, E., Long, F., Mace, K., Magrans de Abril, I., Mochizuki, C., Nayan, C., North, K., Ng, L., Ocker, G. K., Oliver, M., Rhoads, P., Ronellenfitch, K., Schelonka, K., Sevigny, J., Sullivan, D., Sutton, B., Swapp, J., Nguyen, T. K., Waughman, X., Wilkes, J., Wang, M., Farrell, C., Wakeman, W., Zeng, H., Phillips, J., Mihalas, S., Arkhipov, A., Koch, C., and Olsen, S. R. (2023). Stimulus novelty uncovers coding diversity in visual cortical circuits. bioRxiv. doi:10.1101/2023.02.14.528085.